SF2A 2022
J. Richard, A. Siebert, E. Lagadec, N. Lagarde, O. Venot, J. Malzac, J.-B. Marquette, M. N'Diaye, D. Briot (eds)

A LEPTO-HADRONIC JET-FLOW MODEL FOR THE MULTI-WAVELENGTH SED OF M87

M. Boughelilba[1], A. Reimer[1] and L. Merten[1,2]

Abstract. The low-luminosity Active Galactic Nuclei M87, archetype of Fanaroff-Riley I radio-galaxies, was observed in a historically quiet state in 2017. While one-zone leptonic jet models cannot explain the radio-to-gamma-ray spectrum, we explore a hybrid jet-disc scenario. In this work, we model the overall spectral energy distribution of M87s core with a dominating one-zone lepto-hadronic jet numerical emission model, coupled with the contribution from an advection-dominated accretion flow. We find sets of parameter values for which the jet component fits the radio-to-optical data as well as the gamma-ray band. These imply that a mildly relativistic $\delta_{\rm j} = 2.3$, compact emission region of $\sim 5\ r_g$ is suitable to model the contribution of the jet. Given the jet component that we found, we are able to model the remaining X-ray observations with the accretion flow described by a set of parameters that we explored thoroughly. The crucial observational difference between purely leptonic models and lepto-hadronic ones such as ours is the production of neutrinos associated with photo-meson interaction. Thus we also calculate the predicted neutrino flux produced by such scenarios, although it remains below the current instruments sensitivity.

Keywords: Jets, Particle Active Galactic Nuclei, High-energy astrophysics, gamma-ray sources

1 Introduction

M87 is one of the closest examples of low-luminosity Active Galactic Nuclei (AGN), located at a distance of ~ 16.8 Mpc from Earth (corresponding to a redshift $z \approx 0.004$). It hosts a supermassive black hole with a mass $\sim 6.5 \times 10^9 \mathrm{M}_\odot$ (Event Horizon Telescope Collaboration et al. 2019a). For nearly 2 months in 2017, an extensive multi-wavelength observation campaign took quasi-simultaneous data of M87's core region (EHT MWL Science Working Group et al. 2021). The AGN was observed in a particularly low and quiet state. This allows to study the innermost radiation from the AGN, in particular the launching region of the jet, that M87 exhibits, as efforts were made to focus the observation on the core region. Different emission models are usually invoked to explain the spectral energy distribution (SED) of AGN. Among them are lepto-hadronic jet models (e.g. Reimer et al. 2004). In such models, accelerated protons are also present in the jet together with electrons, and the high-energy part of the SED is assumed to be the result of proton-initiated processes, while the low-energy part is due to electron synchrotron emission. A clear observational signature of this type of model is the production of neutrinos. In this work, described in more detail in Boughelilba et al. (2022), we explore a global model, coupling the jet lepto-hadronic emission and the accretion flow, to explain the observed SED of M87. With this model, all the emission would originate from the core region of the AGN.

2 Jet model

In this work, we explore models that can reproduce the quiet and steady state of M87's core observed between March and May 2017. Among the different types of jet, we consider the jet emission region as a spherical blob with a constant radius $r'_{\rm em}$ of magnetized plasma moving at a mildly relativistic speed along the axis of a, during the observation time, non-expanding jet, inclined by an angle θ with respect to the line of sight. This defines a Doppler factor $\delta_{\rm j} = \Gamma_{\rm j}^{-1}(1 - \beta_{\rm j}\cos\theta)^{-1}$ where $\Gamma_{\rm j}$ and $\beta_{\rm j}c$ are the bulk Lorentz factor and velocity respectively.

[1] Institute for Astro and Particle Physics, University of Innsbruck, 6020 Innsbruck, Austria
[2] Ruhr-Universitt Bochum, Institut fr Theoretische Physik IV, 44801 Bochum, Germany

The EHT observation provides a strong constraint on the size of the emission region, as the angular resolution allows to probe the closest regions to the black hole. At 230 GHz, the radio flux was measured with an angular resolution $\theta_{\rm obs}$ of 0.06", corresponding to 7.5 $r_{\rm g}$ (for M87, $r_{\rm g} = GM_{\rm BH}/c^2 \approx 9.8 \times 10^{14}$ cm) in radius. Furthermore, the SED of M87 indicates a self-absorbed, stratified jet below at least 86 GHz (EHT MWL Science Working Group et al. 2021; Blandford & Königl 1979). This lower limit on the self-absorption frequency $\nu_{\rm ssa,obs}$ and corresponding flux $S_{\nu_{\rm ssa,obs}}$ coupled with the estimate of the size of the emission region allows to derive a relation for the magnetic field strength B required. Following the treatment by Kino et al. (2014) for a moving blob, we estimate an order of magnitude for the magnetic field strength between $\sim 5 - 60$ G.

We assume that the emission region contains primary relativistic electrons and protons that are isotropically and homogeneously distributed in the comoving jet frame, and following a power-law energy spectrum cutting off exponentially, such that the spectral number density $n'_{e,p}(E') \propto E'^{-p_{e,p}} e^{-E'/E'_{{\rm max},e,p}}$ cm^{-3}, for $E' \geq E'_{{\rm min},e,p}$ (where e,p denotes the electrons or the protons, respectively). These primary particles are injected continuously into the emission region at a rate q_i (cm^{-3}s^{-1}), where they suffer from different interactions. These are photo-meson production, Bethe-Heitler pair-production, inverse-Compton scattering, γ-γ pair production, decay of all unstable particles, synchrotron radiation (from electrons and positrons, protons, and $\pi^{\pm}$, $\mu^{\pm}$ and $K^{\pm}$ before their respective decays) and particle escape.

To compute the time-dependent direct emission and cascade component from the jet's particles, we use a particle and radiation transport code (see, e.g. Reimer et al. (2019)) that is based on the matrix multiplication method described in Protheroe & Stanev (1993) and Protheroe & Johnson (1996).

All the calculations listed above are done in the jet frame. For a moving blob the observed spectrum νF_ν is then given by the frame transformation $F_\nu = (1+z)\delta_{\rm j}^3 L'_\nu/(4\pi d_{\rm L}^2)$ where L'_ν is the comoving luminosity from the jet with $d_{\rm L} = 16.8$ Mpc the luminosity distance of the source and $\nu_{\rm obs} = \delta_{\rm j}\nu'/(1+z)$. The effect of gamma-ray absorption by the Extragalactic Background Light (EBL) on the escaping photon beam travelling from the source to Earth is taken into account. However, we find that due to the distance of M87, the effects of gamma-ray absorption are negligible for gamma rays with an energy lower than 10 TeV ($\sim 10^{27}$ Hz). As we predict the emitted flux to peak at $\sim 10^{24-25}$ Hz with a strong flux decrease towards higher energies (see Section 4), we hence cannot discriminate between any of the three models.

3 Accretion flow

Low-luminosity AGNs like M87, are expected to host advection-dominated accretion flows around their SMBH (ADAFs, e.g. Rees et al. 1982; Narayan & Yi 1995). ADAFs exist only when the accretion rate is sufficiently low ($\dot{M} \leq 0.01 \dot{M}_{\rm Edd}$), and consist of a two-temperature plasma where the ion temperature is related to the electron temperature through $T_i + 1.08 T_e \approx 6.66 \times 10^{12}\, \beta r^{-1}$ (Narayan & Yi 1995), where β is the ratio between the gas and the total pressure and B is the isotropically tangled magnetic field. In addition to the ADAF, we assume the existence of a truncated standard thin accretion disc (Shakura & Sunyaev disc, Shakura & Sunyaev 1973) extending the outer parts of the ADAF.

In the following, we use the normalized quantities $r = R/R_{\rm S}$, with $R_{\rm S}$ the Schwarzschild's radius and $\dot{m} = \dot{M}/\dot{M}_{\rm Edd}$, with $\dot{M}_{\rm Edd}$ the Eddington accretion rate. We make use of the one-zone, height-integrated, self-similar solutions of the slim disc equations derived by Narayan & Yi (1995) to describe the hot plasma.

To obtain the spectrum emitted by an ADAF, the balance between the heating and cooling of the thermalized electrons present in the plasma is solved to determine the scaled electron temperature $\theta_e = k_B T_e/m_e c^2$. The emission mechanisms that we consider are synchrotron radiation, bremsstrahlung and Comptonization of the two previous components. The total cooling rate is the sum of the three individual cooling rates. The heating mechanisms consist of Coulomb collision between ions and electrons, and viscous energy dissipation. Furthermore, we take $\dot{m}$ of the form $\dot{m} = \dot{m}_{\rm out}\,(r/r_{\rm out})^s$, where $r_{\rm out}$ is the outer radius of the ADAF and is associated with an accretion rate $\dot{m}_{\rm out}$, and s is a mass-loss parameter (introduced by (Blandford & Begelman 1999)) that is used to include the presence of outflows or winds from the ADAF.

The self-similar solutions give a good estimate for the ADAF emission for sufficiently large radii ($r \gg r_{\rm sonic}$, where $r_{\rm sonic}$ is the sonic radius; Narayan et al. 1997), however the inner part of the ADAF ($r \sim 2.5-4$) is thought to be at the origin of the ring observed by the EHT collaboration (Event Horizon Telescope Collaboration et al. 2019b) at 230 GHz. We cannot use the self-similar solutions to account for this inner part emission, but, considering the ADAF framework, we expect that synchrotron radiation is the dominant process in this region. The synchrotron radiation is self-absorbed until the peak frequency corresponding to the emission radius (here 230 GHz at $r \sim 2.5 - 4$ corresponds to $R \sim 5 - 8\, r_g$), hence we add a power-law component $F_\nu \propto \nu^{5/2}$ that we

scale to the observed flux at 230 GHz, to the existing ADAF spectrum (coming from regions $r \geq 5$).

The maximum radius $r_{\rm max}$ is poorly constrained. As there is no evidence for the presence of a truncated thin disc in the infrared data, we set $r_{\rm max} = 2 \times 10^5$ so that any contribution from an outer disc truncated at this radius would be negligible. This value is consistent with the Bondi radius derived by Asada & Nakamura (2012). For the remaining parameters, we explore a broad range of values, and find that the best set is obtained for: $\alpha = 0.1$, $\beta = 0.9$, $\dot{m}_{\rm out} = 1.6 \times 10^{-3}$, $s = 0.39$ and $\delta_e = 10^{-3}$, where α is the viscosity parameter introduced by Shakura & Sunyaev (1973) and δ_e is the fraction of viscous energy directly transmitted to the plasma electrons. With this, the value of the accretion rate in the innermost regions $r \sim 2.5$ is set to the value inferred from the black hole ring observations (Event Horizon Telescope Collaboration et al. 2019b), namely $\dot{m} \sim 2 \times 10^{-5}$. The values of β and the electron density in the black hole vicinity are compatible with values derived for MAD (Magnetically Arrested Disk; see e.g. Bisnovatyi-Kogan & Ruzmaikin 1976; Narayan et al. 2003) simulations (Event Horizon Telescope Collaboration et al. 2021). The ADAF component alone is not entirely consistent with the X-ray data, however its contribution is added to the jet emission to produce the overall SED (see Section 4).

4 Results

We investigate whether the total joint model (jet component added to the ADAF component) can explain the global SED. We start by setting the fixed parameters of the jet. Since the synchrotron self-absorption frequency is a critical feature of the observed spectrum (see Section 2), we fix the size of the emission region in order to maximise the self-absorption frequency value, while being consistent with the measured Event Horizon Telescope Collaboration et al. (2019c) flux value, namely we set $r'_{\rm em} = 5 \times 10^{15}$ cm $\approx 5\, r_g$. We use a Doppler factor $\delta_j \approx 2.3$. This corresponds to a velocity $\beta c = 0.73c$ with an inclination of the jet $\theta = 17°$ The SED is obtained by averaging the light curves over a time corresponding to the observation campaign time, i.e. 2 months. The goodness of the fits (for both the light curve and the SED) is estimated by computing the p-value of the χ^2-test for each model. We keep models that have a p-value $p_{\chi^2} > 0.01$.

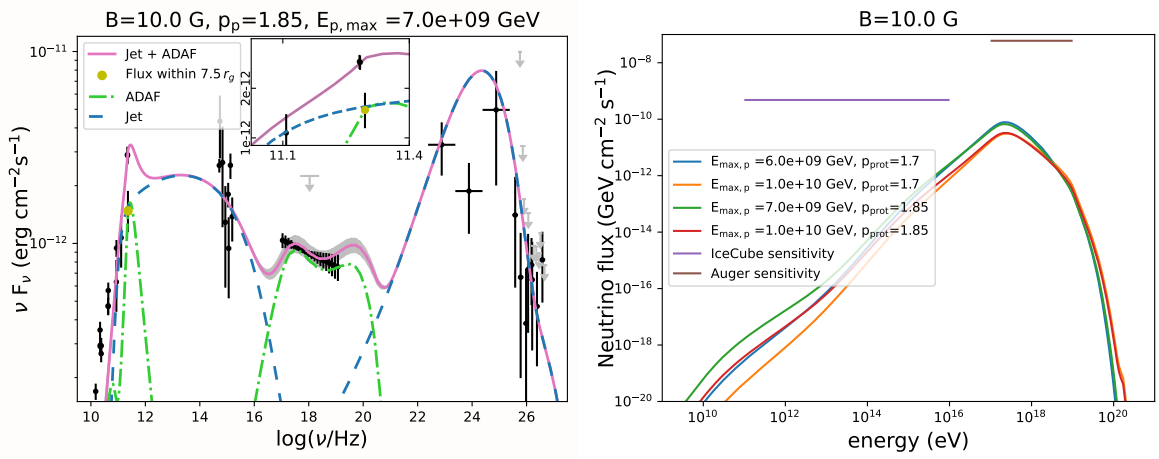

Fig. 1. Left: Global core emission (pink line), composed of the jet emission (blue dashed curve) and the ADAF emission (green dadh-dotted curve), for a proton spectral index $p_{\rm p} = 1.85$ and maximum proton energy $E_{\rm p,max} = 7 \times 10^9$ GeV, for a magnetic field of 10 G. **Right:** Predicted neutrino spectra for the models with $B = 10$ G.

In the left panel of Figure 1 we present one of the models, for which $B = 10$ G and $p_{\rm p} = 1.85$. For $B = 10$ G, good fits are obtained when the proton spectral index ranges from $p_{\rm p} = 1.7$ to $p_{\rm p} = 1.85$ and the maximum proton energy from $E_{\rm p,max} = 6 - 7 \times 10^9$ GeV to $E_{\rm p,max} = 10 \times 10^9$ GeV. We obtain a jet power of $P_{\rm j} = 2 - 4 \times 10^{43}\,{\rm erg\,s^{-1}}$ and ratios of magnetic-to-particle energy density of $U_{\rm part}/U_B = 0.6 - 1.3$. For $B = 50$ G we find that it is harder to fit the data, and one has to consider lower proton densities and higher maximum proton energies. For a proton injection spectrum of $p_{\rm p} = 1.7 - 2$, we find a good fit only for maximum proton energies $E_{\rm p,max} \geq 7 - 8 \times 10^9$ GeV. With these models we obtain a jet power of $P_{\rm j} \approx 3 \times 10^{44}\,{\rm erg\,s^{-1}}$ and ratios of magnetic energy density to particle energy density of $U_{\rm part}/U_B \approx 10^{-2}$

The neutrino spectra (single-flavor flux) produced by the source from the models with $B = 10$ G are presented

in the right panel of Figure 1. The predicted flux is low, because the main gamma-ray emission contribution is due to proton synchrotron radiation, which does not produce neutrinos. We compare this value to the sensitivity to a point-like source of high-energy neutrinos with a neutrino flux $\propto E^{-2}$, of the Pierre Auger Observatory (Aab et al. 2019) and the IceCube observatory (Aartsen et al. 2017) at M87's declination.

5 Conclusion

We have successfully applied a lepto-hadronic, time-dependent jet model, complemented with an advection dominated accretion flow to M87's nuclear emission in a low flux state. We found a range of parameter values that allow to reproduce the multi-wavelength data taken in 2017 during the EHT MWL Science Working Group et al. (2021) observation campaign. We focused on an jet emission region of the size similar to the EHT angular resolution at M87's distance, namely $5r_{\rm g}$. Within this region we estimated a magnetic field strength in the range 5-60 G. For a range $10\,{\rm G} \leq B \leq 50\,{\rm G}$ we found that the electrons spectral index is limited to $p_e \approx 1.80 - 1.85$, in order to reproduce the radio-to-optical part of the SED. For the same reason, the maximum energy for the electron distribution is found to be $E_{{\rm max},e} \leq 5$ GeV. Concerning the high energy emission, we have found parameter values that fit the data for the whole range of magnetic field strengths considered. However, it it worth pointing out that the proton maximum energy and spectral index ranges are dependent on the value for the magnetic field strength. For $B = 10$ G we found that when $p_p \simeq 1.7$ (minimum proton spectral index) the proton maximum energy is in the range $6 \times 10^9\,{\rm GeV} \leq E_{{\rm max},p} \leq 1 \times 10^{10}\,{\rm GeV}$ while for $p_p \simeq 1.85$ (maximum proton spectral index for these parameter values) it is in the range $7 \times 10^9\,{\rm GeV} \leq E_{{\rm max},p} \leq 1 \times 10^{10}\,{\rm GeV}$. For $B = 50$ G when $p_p \simeq 1.7$ (minimum proton spectral index) the proton maximum energy is in the range $7 \times 10^9\,{\rm GeV} \leq E_{{\rm max},p} \leq 1 \times 10^{10}\,{\rm GeV}$ while for $p_p \simeq 2.00$ (maximum proton spectral index for these parameter values) it is in the range $8 \times 10^9\,{\rm GeV} \leq E_{{\rm max},p} \leq 1 \times 10^{10}\,{\rm GeV}$.

MB has for this project received funding from the European Unions Horizon 2020 research and innovation program under the Marie Sklodowska-Curie grant agreement No 847476. The views and opinions expressed herein do not necessarily reflect those of the European Commission. LM acknowledges support from the DFG within the Collaborative Research Center SFB1491 "Cosmic Interacting Matters - From Source to Signal". This research was funded in part by the Austrian Science Fund (FWF) (grant number I 4144-N27).

References

Aab, A., Abreu, P., Aglietta, M., et al. 2019, J. Cosmology Astropart. Phys., 2019, 004
Aartsen, M. G., Abraham, K., Ackermann, M., et al. 2017, ApJ, 835, 151
Asada, K. & Nakamura, M. 2012, ApJ, 745, L28
Bisnovatyi-Kogan, G. S. & Ruzmaikin, A. A. 1976, Ap&SS, 42, 401
Blandford, R. D. & Begelman, M. C. 1999, MNRAS, 303, L1
Blandford, R. D. & Königl, A. 1979, ApJ, 232, 34
Boughelilba, M., Reimer, A., & Merten, L. 2022, arXiv e-prints, arXiv:2208.14756
EHT MWL Science Working Group, Algaba, J. C., Anczarski, J., et al. 2021, ApJ, 911, L11
Event Horizon Telescope Collaboration, Akiyama, K., Alberdi, A., et al. 2019a, ApJ, 875, L6
Event Horizon Telescope Collaboration, Akiyama, K., Alberdi, A., et al. 2019b, ApJ, 875, L5
Event Horizon Telescope Collaboration, Akiyama, K., Alberdi, A., et al. 2019c, ApJ, 875, L1
Event Horizon Telescope Collaboration, Akiyama, K., Algaba, J. C., et al. 2021, ApJ, 910, L13
Kino, M., Takahara, F., Hada, K., & Doi, A. 2014, ApJ, 786, 5
Narayan, R., Igumenshchev, I. V., & Abramowicz, M. A. 2003, PASJ, 55, L69
Narayan, R., Kato, S., & Honma, F. 1997, ApJ, 476, 49
Narayan, R. & Yi, I. 1995, ApJ, 452, 710
Protheroe, R. J. & Johnson, P. A. 1996, Astroparticle Physics, 4, 253
Protheroe, R. J. & Stanev, T. 1993, MNRAS, 264, 191
Rees, M. J., Begelman, M. C., Blandford, R. D., & Phinney, E. S. 1982, Nature, 295, 17
Reimer, A., Böttcher, M., & Buson, S. 2019, ApJ, 881, 46
Reimer, A., Protheroe, R. J., & Donea, A. C. 2004, A&A, 419, 89
Shakura, N. I. & Sunyaev, R. A. 1973, A&A, 500, 33